A Theoretical Procedure for Estimating Saturation Temperature Inside Solar Two-Phase Loops

Khalid Ahmad Joudi [(1)] *and Aouf Abdulrahman Al-Tabbakh* [(2)*]

(1) Department of Mechanical Engineering, College of Engineering, Baghdad University, Iraq.
(2) Department of Mechanical Engineering, College of Engineering, Mustansiriya University, Iraq.

Abstract:

This work presents a theoretical analysis for the prediction of refrigerant saturation temperature inside a typical solar two-phase loop. This loop may be incorporated in any solar heating system for transporting heat between the solar collector and storage tank. The procedure takes into account all influencing parameters such as:- solar irradiance, ambient temperature, heat transfer coefficients in the source (collector) and sink (condenser), collector fill ratio and the geometric parameters of the solar collector and condenser.The trend of change of saturation temperature was studied over a typical daytime period extending 8 hours. Mathematical models were formulated for the collector and condenser to take into account the most influencing parameters. The models are highly interrelated which required an iterative procedure. A computer program was built to implement the iterative procedure and simulate the change of saturation temperature during the studied period. The period was divided into small time intervals of 10 seconds.Results reveal a significant influence of condenser area, collector fill ratio and the working conditions on the calculated saturation temperature. Optimum conversion of energy occurs at a fill ratio of 0.85 at which saturation temperature is about $40^{o}C$ for the system under consideration.

Key words: *Refrigerant saturation temperature, boiling solar collector, Natural circulation loops, thermosyphons.*

<div dir="rtl">

**دراسة نظرية لتخمين درجة حرارة التشبع
داخل الدورات الشمسية ثنائية الطور**

أ.د. خالد احمد الجودي ــ قسم الهندسة الميكانيكية ــكلية الهندسة ــ جامعة بغداد
م.د. عوف عبد الرحمن احمد الطباخ ــ قسم الهندسة الميكانيكية ــكلية الهندسة ــ الجامعة المستنصرية

خلاصة

يتناول هذا البحث دراسة نظرية تهدف إلى تخمين درجة حرارة التشبع لمائع تبريد يجري داخل دورة شمسية نموذجية ثنائية الطور. يمكن استعمال دورات كهذه في أية منظومة تسخين شمسية لغرض نقل الحرارة بين المجمع الشمسي وخزان الماء. وقد جرى في هذه الطريقة تناول كل العوامل المؤثرة على الأداء مثل :- شدة الإشعاع الشمسي ودرجة حرارة الجو ومعاملات انتقال الحرارة في المجمع والمكثف إضافة إلى نسبة ملىء المجمع وأبعاده مع أبعاد المكثف تم دراسة نمط تغير درجة حرارة التشبع خلال فترة نهارية نموذجية تمتد 8 ساعات حيث تم صياغة نماذج رياضية لتمثيل كل من المجمع

</div>

الشمسي والمكثف تشتمل معظم العوامل الرئيسية المؤثرة على الأداء . إن النماذج الرياضية متداخلة مع بعضها مما يوجب إيجاد حل يعتمد التجربة والخطأ . لذا تم بناء برنامج حاسوبي لحل هذه المسألة المترابطة حلا يعتمد التجربة والخطأ ويخمن درجة حرارة التشبع للمائع الشغال خلال فترة المحاكاة النظرية السالفة الذكر . وقد تم تقسيم الفترة إلى فترات قصيرة بطول 10 ثواني.أظهرت النتائج تأثيرا ملحوظا لكل من مساحة المك   ثف ونسبة ملىء المجمع وظروف التشغيل على القيمة المحسوبة لدرجة حرارة التشبع . وظهر ان التحويل الأمثل للطاقة يتم عند نسبة ملىء   0.85 ودرجة حرارة تشبع مقدارها 40 درجة مئوية للمنظومة قيد الدراسة.

*Corresponding author, e-mail: aoufaltabbakh@yahoo.com
Phone: +9647703440722

Nomenclature:

Symbol	Meaning	Units
A_1	Collector subcooled area	m^2
A_2	Collector boiling area	m^2
A_3	Collector superheated area	m^2
A_4	Condensation area	m^2
A_{4o}	Outside wall area of the condensation region	m^2
A_5	Condenser subcooled area	m^2
A_{5o}	Outside wall area of condenser subcooled region	m^2
A_c	Collector area	m^2
A_{co}	Condenser area	m^2
A_{co2}	Condenser wall outside area	m^2
A_t	Water storage tank outside surface area	m^2
c_p	Specific heat	$kJ/(kg\ ^oC)$
c_{pw}	Water specific heat at constant pressure	$kJ/(kg\ ^oC)$
D	Collector pipe inside diameter	m
D_c	Condenser pipe inside hydraulic diameter	m
D_{co}	Condenser pipe outside hydraulic diameter	m
D_o	Collector pipe outside diameter	m
F_1	Collector efficiency factor for the subcooled region	
F_2	Collector efficiency factor for the boiling region	
F_3	Collector efficiency factor for the superheated region	
F_f	Absorber plate fin efficiency	
FL	Collector fill ratio	
F_{Rv}	Collector heat removal factor in the superheated region	
h_1	Liquid heat transfer coefficient inside collector pipes	$W/(m^2\ ^oC)$
h_3	Vapor heat transfer coefficient inside collector pipes	$W/(m^2\ ^oC)$
h_b	Boiling heat transfer coefficient	$W/(m^2\ ^oC)$
h_c	Condensation heat transfer coefficient	$W/(m^2\ ^oC)$
h_{cm}	Modified condensation heat transfer coefficient	$W/(m^2\ ^oC)$
h_{fg}	Latent heat of vaporization	kJ/kg
I_T	Solar radiation intensity	W/m^2

k	thermal conductivity	
k_b	Collector bond material thermal conductivity	W/(m ^{o}C)
L_1	Length of the collector subcooled region	m
L_3	Length of the collector superheated region	m
L_4	Condensation region height	m
LT	Local Time	hr
$\dot{m}$	Refrigerant mass flow rate	kg/s
$\dot{m}_w$	Tank water withdrawal rate	kg/s
M_w	Tank Water mass	kg
n	Number of collector pipes	
n_c	Number of condenser pipes	
n_τ	Number of time intervals in the simulation period	
P_{ci}	Condenser pipe inside perimeter	m
P_{co}	Condenser pipe outside perimeter	m
Pr	Prandtl number $= \dfrac{\mu c_p}{k}$	
q_b	Boiling heat flux	W/m^2
Q_1	Useful heat gain in the collector subcooled region	W
Q_2	Useful heat gain in the collector boiling region	W
Q_3	Useful heat gain in the collector superheated region	W
Q_4	Heat rejection rate in the condensation region	W
Q_5	Heat rejection rate in the condenser subcooled region	W
Q_l	Heat lost to the environment by the water storage tank	W
Q_w	Rate of heat lost by the water withdrawn from the tank	W
Re	Reynolds number $= \dfrac{\rho VD}{\mu}$	
T_1	Collector inlet temperature	^{o}C
T_2	Collector exit temperature	^{o}C
T_a	Ambient temperature	^{o}C
T_{cw}	Condenser pipe wall temperature	^{o}C
T_l	Compensation water temperature	^{o}C
T_s	Saturation temperature	^{o}C
T_{st}	Stagnation temperature	^{o}C
T_{t1}	Tank water temperature at the start of time interval	^{o}C
T_{t2}	Tank water temperature at the end of time interval	^{o}C
T_w	Collector pipe inside wall temperature	^{o}C
U_1	Collector top heat loss coefficient in the subcooled region	W/(m^2 ^{o}C)
U_2	Collector top heat loss coefficient in the boiling region	W/(m^2 ^{o}C)
U_3	Collector top heat loss coefficient in the superheated region	W/(m^2 ^{o}C)
U_t	Tank overall heat loss coefficient	W/(m^2 ^{o}C)

W	Distance between collector pipes	m

Greek symbol	**Meaning**	**Units**
δ_b	Collector bond thickness	m
η_i	Loop instantaneous efficiency	
μ	Absolute viscosity	kg/(m s)
ρ	Density	kg/m^3
σ	Surface tension	m^2/s
τ	Time	s
$\tau\alpha$	Collector transmittance-absorptance product	
Δ	Difference	
Ψ	Two-phase loop overall factor	

Subscript	**Meaning**
l	Liquid
v	Vapor
w	Water or wall

Introduction

Natural circulation loops (sometimes referred to as thermosyphons) are effective devices for transporting heat between a source and a sink. The source may be a solar collector of a solar heating system and the sink is the water storage tank. If a boiling refrigerant is employed as a working fluid inside the loop, a condenser should then be installed inside the water storage tank to retrieve the heat absorbed by the collector. The refrigerant in such a solar two-phase loop is circulated in a confined pipes sealed from the atmospheric pressure. It boils in the collector upon the exposure to solar radiation and condenses in the condenser, flowing back to the starting point at the collector inlet to complete the loop. This configuration makes the saturation pressure and temperature functions of boiling and condensation rates, thus functions of operation conditions and system geometry. The solar collector is partly filled with a boiling fluid or refrigerant. The collector fill ratio is defined as the volume of the collector pipes filled with the working fluid to the total collector pipes volume.

The work in boiling collectors started experimentally in the late seventies of the last century with the work of Soin et al. [1] who studied a thermosyphon boiling solar collector containing an acetone and petroleum ether mixture. They developed a modified form of the well known Hottel–Whillier–Woertz-Bliss (HWWB) equation which would account for the fraction of the liquid in a particular collector. Downing and Walden [2] experimentally studied the heat transfer processes in boiling solar domestic hot water systems using R-11 and R-114. They concluded that phase change heat transfer fluids operate with better efficiency and faster response than

circulating liquids in single phase solar collectors. Schreyer [3] experimentally investigated the use of a thermosyphon refrigerant R-11 charged solar collector for residential applications. He found that for two identical collectors, the peak instantaneous efficiency of a boiling refrigerant charged collector was 6 percent greater than that of a hydronic fluid circulating solar collector.

A detailed study of boiling fluid solar collectors was done by Al-Tamimi and Clark [4]. They tested a boiling collector containing R-11 and developed an analytical model to investigate the effect of subcooling and the liquid level on collector efficiency. They defined the factor Z^* to be the fraction of the collector required to heat the fluid to its boiling temperature. Al-Assy and Clark [5] generalized the analysis of Al-Tamimi and Clark to include the superheated portion of the boiling collector. They introduced another factor Z^{**} to account for the superheated portion of a boiling collector. Further theoretical analyses of a flat-plate solar collector with internal boiling were presented by references [6] and [7].

The above studies concentrated on the thermal behavior of the boiling solar collector alone regardless of the other components of the thermosyphon loop such as the condenser and the connecting pipes. Fanney and Terlizzi [8] conducted experiments on a complete two-phase thermosyphon hot water system charged with a refrigerant. Radhwan et. al. [9] investigated two R-11 charged integrated solar water heaters for forced and natural circulation water flows. The results showed that the inclination of the condenser integrated within the collector frame had a remarkable effect for natural circulation water flow, while it had no significant effect for forced circulation flow.

Pluta and pomierny [10] conducted a theoretical and experimental study on a phase change solar thermosyphon charged with R-22. The analysis assumed that all the collector is at saturation temperature. Joudi and Al-Tabbakh [11] conducted a theoretical study on a two-phase thermosyphon solar domestic hot water system using R-11. The study utilized a computer simulation program for a typical daytime period divided into equal intervals of 15 minutes. Simulations were conducted for no loading, continuous loading and intermittent loading. The effects of changing collector fill ratio and condenser area were not considered in that study. Lin et al. [12] employed alcohol as working fluid in the thermosyphon loop whereas, Esen and Esen [13] experimented with three identical two-phase thermosyphon solar heaters charged with R-134a, R407C and R410A. The system with R410A gave the best performance for both non loading and loading operation.

All studies mentioned above considered the saturation temperature along with mass flow rate as input values and known in advance. This assumption, of course, is not applicable in any closed natural circulation loop wither it is solar or not. The present work seeks to theoretically analyze a solar natural circulation (thermosyphon) loop to estimate the saturation temperature changes during a specified daytime period. The correct estimation of the saturation temperature is a key factor in studying the overall performance of any solar heating system incorporating a two-phase thermosyphon. The analysis also entails a prediction of the working fluid mass flow rate. A computer program is used to perform the calculation which are highly interrelated

requiring subtle iterative procedure. The program tracks the change in saturation temperature at intervals of 10 seconds. Steady-state thermal models are used at each consecutive step.

2. Loop Description

The two-phase solar loop under consideration consists of the following components; the boiling flat-plate solar collector, the upriser, the condenser, and the downcomer as shown in Fig.1. The solar collector is a flat-plate conventional type having 10 parallel pipes. Refrigerant R-123 is circulated in the collector pipes. The temperature of the refrigerant increases while flowing inside the hot pipes. When the refrigerant temperature reaches the saturation temperature, boiling commences, and the vapor refrigerant rises in the remaining length of the pipes, passing through the upriser and then to the condenser which is located inside the storage tank.
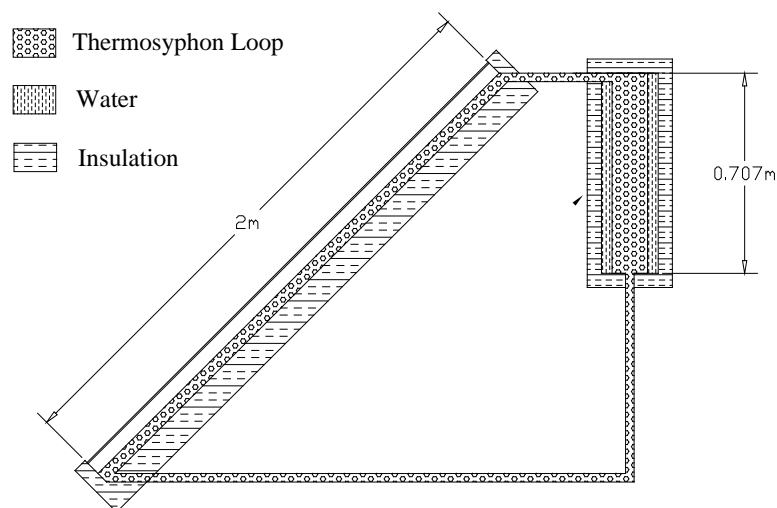
Fig. (1) Schematic vie͘w of the two-phase thermosyphon solar loop.

The condenser is composed of several parallel pipes of rectangular cross-section measuring (80×20) mm. These rectangular pipes are inserted vertically inside a rectangular storage tank. The condenser area used in the simulation is 0.63 m^2 for a condenser having 5 pipes. The effect of varying the condenser area was achieved by increasing the number of pipes and keeping pipe dimensions constant. Table 1 shows the dimensions and characteristics of the system under consideration.

Table (1): System dimensions and characteristics.

Collector	Dimensions (width×length)	1×2	m
	Top heat loss coefficient	4.5	W/(m^2 ^{o}C)
	Transmittance-absorptance	0.85	
	Fill ratio	0.05 to 0.95	
	Inside pipe diameter	0.01	m
	Outside pipe diameter	0.012	m
	Pipe length	2	m
	Pipe spacing	0.1	m
	Number of pipes	10	
	Absorber plate thickness	0.001	m
	Absorber plate material	copper	
	Tilt angle	45°	
Tank	Total volume	0.10828	m^3
	Outside surface area	3.187	m
	Heat loss coefficient	0.5	W/(m^2 ^{o}C)
Condenser	Inside area	0.63	m^2
	Dimensions (width×length)	0.02×0.08	m
	Number of condenser pipes	5 to 20	
	Inside perimeter	0.178	m
	Pipe thickness	0.001	m

The refrigerant undergoes sensible heating, boiling or latent heat transfer, and superheating of the vapor in the collector. Similar modes are encountered in the condenser, but in the opposite sequence. The vapor condenses inside the condenser pipes and the liquid refrigerant is returned back to the collector via the downcomer. The refrigerant in the loop is confined and the pressure inside the loop will depend on the prevailing saturation temperature. This temperature is a function of the collector and condenser average temperatures, the amount of refrigerant, and the solar radiation intensity.

3. Assumptions used in the theoretical model

To analyze the heat transfer problem around the two-phase solar loop, the following assumptions have been made:-
1. Frictional pressure losses in the pipes are ignored.
2. The upriser and the downcomer are assumed to be well insulated and the thermal losses from these components are ignored.

3. The liquid level is the same in the source (collector) and the sink (condenser and/or downcomer).

4. The liquid height in the collector remains constant during the whole simulation period. This height is divided into two sub-regions; the lower part is for sensible heating of the liquid refrigerant, and the remaining part is for boiling.

5. All the useful energy received in the collector (sensible + latent) is assumed to be delivered to the water storage tank via the condenser.

6. The saturation temperature is constant throughout the loop at each time interval. A change of phase occurs whenever the refrigerant temperature reaches this value, whether in the collector or condenser.

4. Thermal analysis of the two-phase flat-plate solar collector

For the sake of simplifying the analysis; The two-phase solar collector is divided into three regions (Fig. 2). The subcooled lower region, the boiling mid region, followed by the upper superheated region. Any increase in the subcooled region means a decrease in the boiling region and vice versa.
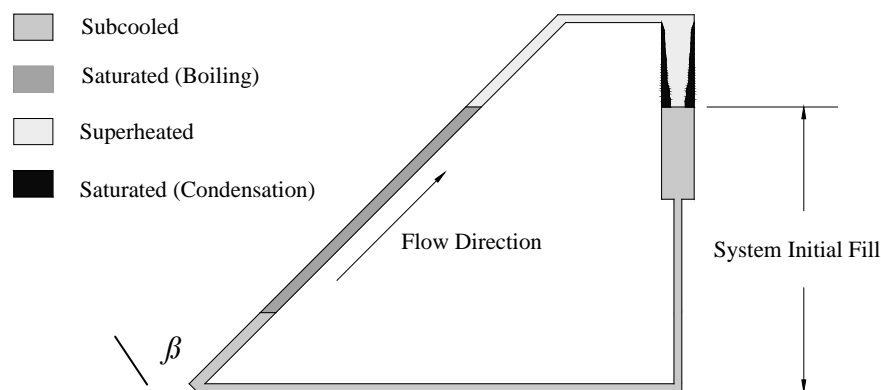
Fig. (2) Heat transfer regions.

The solar radiation intensity incident on the solar collector is calculated using the standard ASHRAE model [14]. The 21st day of December was chosen as a representative day of the heating season. The variation of the ambient temperature during the simulation period for 21st of December was approximated by the following sine function, given in degrees centigrade [11]:-

$$T_a = 10 + 15\sin\left(\frac{\pi(LT-8)}{8}\right) \tag{1}$$

Where LT is the local time in 24 hour clock. Equation (1) is valid between 8 a.m. to 16 p.m. which is the duration of the simulation period.

4.1 Subcooled region

The working fluid enters the collector as a subcooled liquid at a temperature T_1 . If the saturation temperature T_s is known, then the collector area required to reach T_s , which also represents the area of the subcooled region, is estimated by the following equation adapted from reference [7]:-

$$A_1 = \frac{\dot{m}c_{pl}}{U_1 F_1} \ln \frac{I_T \tau \alpha - U_1 (T_1 - T_a)}{I_T \tau \alpha - U_1 (T_s - T_a)} \qquad (2)$$

The parameters T_1 , T_s , $\dot{m}$, and U_1 in the above equation are not known in advance. Initial guess values of these parameters are assumed at the beginning of the simulation process. The values should be modified later and the whole calculations are repeated until an acceptable tolerance of 0.0001 between the guessed and calculated values is achieved.

The useful heat gain of the subcooled region is estimated by the following equation:-

$$Q_1 = \dot{m}c_{pl}(T_s - T_1) \qquad (3)$$

F_1 is the collector efficiency factor of the subcooled region. It is calculated using the following equation [15]:-

$$F_1 = \frac{\dfrac{1}{U_1 W}}{\dfrac{1}{U_1 \left[D_o + F_f (W - D_o) \right]} + \dfrac{2\delta_b}{k_b D_o} + \dfrac{1}{\pi D h_1}} \qquad (4)$$

Where W is the distance between collector risers and h_1 is the convective heat transfer coefficient inside the risers calculated by the following formulas [18]:-

$$h_1 = h_l = 2.776 \left(\frac{k}{D} \right) \left(\text{Re}\,\text{Pr}\,\frac{D}{L_1} \right)^{1/3} \text{ for laminar flow (Re} < 2000) \qquad (5)$$

$$h_1 = h_t = 0.023 \left(\frac{k}{D} \right) \text{Re}^{0.8}\,\text{Pr}^{1/3} \quad \text{for turbulent flow (Re} > 2300) \qquad (6)$$

$$h_1 = h_{tr} = \frac{h_l + h_t}{2} \qquad \text{for transitional flow } (2000 \leq \text{Re} \leq 2300) \qquad (7)$$

Where Re is the Reynolds number based on the collector pipe inner diameter D and the subcooled length L_1 . Pr is the Prandtl number. The value of Re in the subcooled region lies in the laminar region during most of the simulation period while the turbulent mode dominates the superheated region.

4.2 Boiling region

Once the subcooled region area A_1 is estimated, the boiling region area can be directly estimated as follows:-

$$A_2 = FL \times A_c - A_1 \qquad (8)$$

Where FL is the collector fill ratio and A_c is the collector total area. The useful heat gain in the boiling region which is a function of A_2 can be calculated by the following equation adapted from [5]:-

$$Q_2 = F_2 A_2 \left[I_T \tau \alpha - U_2 (T_s - T_a) \right] \qquad (9)$$

The rate of boiling which equals the working fluid mass flow rate is then calculated by the following equation:-

$$\dot{m} = \frac{Q_2}{h_{fg}} \qquad (10)$$

The value of $\dot{m}$ calculated from the above equation should be compared with the guessed value used in the previous calculations. If they differ, the whole calculation is repeated using the new value. F_2 is the collector efficiency factor for the boiling region. It is calculated using the following equation [15]:-

$$F_2 = \frac{\dfrac{1}{U_2 W}}{\dfrac{1}{U_2 \left[D_o + F_f (W - D_o) \right]} + \dfrac{2\delta_b}{k_b D_o} + \dfrac{1}{\pi D h_b}} \qquad (11)$$

h_b is the boiling heat transfer coefficient inside the collector pipes calculated using Rohsenow's formula [19]:-

$$h_b = \left(\frac{\mu_l h_{fg}}{T_w - T_s}\right)\left(\frac{9.81(\rho_l - \rho_v)}{\sigma}\right)^{0.5}\left(\frac{c_{pl}(T_w - T_s)}{0.01 h_{fg}\left(\frac{\mu_l c_{pl}}{k_l}\right)^{1.7}}\right)^{1.8} \tag{12}$$

Where T_w is the collector pipe inside wall temperature and is calculated by considering it as the collector absorber plate mean temperature.

4.3 Superheated region

The remaining area of the collector which is not filled with the refrigerant depends on the initial fill ratio. It is estimated by the following equation:-

$$A_3 = A_c (1 - FL) \tag{13}$$

The length of the superheated part along one of the collector risers (L_3) is calculated by the following equation:-

$$L_3 = \frac{A_3}{nW} \tag{14}$$

Where n is the number of collector risers and W is the distance between the risers. The collector exit temperature of the working fluid can now be calculated using the following equation:-

$$T_2 = T_s + \frac{Q_3}{\dot{m}c_{pv}} \tag{15}$$

Where Q_3 is the useful heat gain for the superheated region, estimated by the following equation:-

$$Q_3 = F_{Rv}A_3\left[I_T\tau\alpha - U_3(T_s - T_a)\right] \tag{16}$$

F_{Rv} is the collector heat removal factor for the superheated region. It is calculated using the standard Hottel-Whillier-Woertz-Bliss (HWWB) equation adapted for the superheated region:-

$$F_{Rv} = \frac{\dot{m}c_{pv}}{U_3 A_3}\left(1 - \exp\left(\frac{-U_3 A_3 F_3}{\dot{m}c_{pv}}\right)\right) \tag{17}$$

F_3 is the collector efficiency factor for the superheated region, calculated by the following equation [15]:-

$$F_3 = \frac{\dfrac{1}{U_3 W}}{\dfrac{1}{U_3\left[D_o + F_f\left(W - D_o\right)\right]} + \dfrac{2\delta_b}{k_b D_o} + \dfrac{1}{\pi D h_3}} \tag{18}$$

h_3 is the convective heat transfer coefficient of the vapor working fluid in the superheated region. It is estimated by the same formulas used in the subcooled region but by applying vapor properties instead of liquid ones [18].

Collector instantaneous efficiency is defined as the ratio of the useful heat gain of the solar collector to the total rate of solar radiation incident on the solar collector:-

$$\eta_i = \frac{Q_1 + Q_2 + Q_3}{I_T A_c} \tag{19}$$

5. Thermal analysis of the condenser

The condenser will be divided into two regions rather than three. In the first region, near the condenser inlet, superheated vapor enters the condenser and will be desuperheated to the saturation temperature. At the same time, condensation will commence at the condenser inside walls as long as the temperature is below the vapor saturation temperature. So, the working fluid in the first region will encounter two processes; sensible cooling of the incoming vapor, and film condensation at the vertical walls. If the system fill ratio is large enough, the lower part of the condenser will be flooded with liquid refrigerant. This flooded part constitutes the subcooled region of the condenser, which is the second region in the condenser analysis and will depend on the system fill ratio.

5.1 Condensation region

The coexistence of desuperheating and film condensation was studies by Van der Walt and Kroger [16] who suggested a modification to the conventional Nusselt film condensation to take into account the superheated state at the condenser inlet. They suggested a modified condensation heat transfer coefficient given by the following equation:-

$$h_{cm} = h_c \left(1 + \frac{c_{pv}(T_2 - T_s)}{h_{fg}} \right)^{0.25} \tag{20}$$

Where h_c is the conventional film-wise condensation of Nusselt, averaged for the condensation height L_4 , and is given by the following equation:

$$h_c = 0.943 \left(\frac{9.81 \rho_l (\rho_l - \rho_v) h_{fg} k_l^3}{L_4 \mu_l (T_s - T_{cw})} \right)^{0.25} \tag{21}$$

L_4 is measured downward from the condenser inlet and can be estimated by the following equation depending on the collector initial fill:

$$L_4 = L_3 \sin(\beta) \tag{22}$$

The above equation is valid only when part of the condenser is flooded with liquid refrigerant. For the case of non-flooded condenser at low fill ratios, the whole condenser vertical length will be considered available for condensation. The heat rejection to the water tank in the condensation region is found by the following equation:

$$Q_4 = h_c A_4 (T_s - T_{cw}) \tag{23}$$

Where A_4 is the inside surface area of the condenser pipes in the condensation region, and is found by the following equation:-

$$A_4 = L_4 \times n_c \times P_{ci} \tag{24}$$

Where n_c is the number of condenser pipes which is 5 for a condenser having a heat transfer area of 0.63 m^2. P_{ci} is the condenser pipe inside perimeter.

5.2 Subcooled region

When part of the condenser is filled with liquid refrigerant, the remaining area for condensation will decrease, and the working fluid will undergo subcooling in this region. The condenser pipes total inside area available for subcooling is found by the following equation:

$$A_5 = A_{co} - A_4 \tag{25}$$

Where A_{co} is the total inside surface area of the condenser. The working fluid temperature at the end of the subcooled region of the condenser can be evaluated by the following equation [11]:-

$$T_1 = T_{t1} + (T_s - T_{t1}) \exp\left(\frac{-(UA)_5}{\dot{m}c_{pl}}\right) \tag{26}$$

$(UA)_5$ is the product of overall heat transfer coefficient and heat transfer area of the condenser subcooled region, and is given by the following equation:

$$(UA)_5 = \left(\frac{1}{h_1 A_5} + \frac{\ln(D_{co}/D_c)}{2\pi k_c L_5} + \frac{1}{h_w A_{5o}}\right)^{-1} \tag{27}$$

In the same manner, the condenser pipes total outside area in the subcooled region (A_{5o}) is found by the following equation:-

$$A_{5o} = A_{co2} - A_{4o} \tag{28}$$

Where A_{co2} is the total outside surface area of the condenser. A_{4o} is condenser outside area available for condensation and is found by the following equation:-

$$A_{4o} = L_4 \times n_c \times P_{co} \tag{29}$$

Where P_{co} is the condenser pipe outside perimeter. The heat rejection to the water tank in the subcooled region is given by the following equation:

$$Q_5 = \dot{m}c_{pl}(T_s - T_1) \tag{30}$$

The value of T_1 calculated from equation (26) should be compared with the old value used in the previous calculations. If they are different, all the calculations are repeated using the new value until the specified tolerance, of 0.0001 or less, is reached. The equality of the guessed and the calculated collector initial temperature T_1 ensures that the sensible heat balance is satisfied throughout the loop. The latent heat balance will also be satisfied later and this condition will be used to estimate the saturation temperature.

6. The loop saturation temperature

The following reasoning is used to determine the saturation temperature:

$$\begin{pmatrix} latent\ heat\ gain \\ in\ collector \end{pmatrix} = \begin{pmatrix} latent\ heat\ rejection \\ in\ condenser \end{pmatrix} \qquad (31)$$

$$F_2 A_2 \left[I_T \tau\alpha - U_2 (T_s - T_a) \right] = (UA)_4 (T_s - T_{t1}) \qquad (32)$$

The left side of the above equation represents the useful heat gain in the boiling region using the adapted Hottel-Whillier-Woertz-Bliss method [15]. The terms of the equation can be rearranged to get:-

$$\frac{F_2 A_2 U_2}{(UA)_4} \left[\frac{I_T \tau\alpha}{U_2} - T_s + T_a \right] - T_s + T_{t1} = 0 \qquad (33)$$

Define The Loop Overall Factor ψ as:

$$\Psi = \frac{F_2 A_2 U_2}{(UA)_4} \qquad (34)$$

Ψ is a newly-defined factor that combines the geometric and heat transfer aspects of the whole two-phase solar thermosyphon loop.

Substituting ψ in equation (33) and rearranging to get:

$$T_s = \frac{T_{t1} + \Psi T_{st}}{1 + \Psi} \qquad (35)$$

It can be concluded from equation (35) that many loop parameters influence the value of the saturation temperature such as, the solar radiation intensity which appears implicitly in T_{st} which is the collector stagnation temperature of the boiling region defined, the tank temperature T_{t1} , in addition to the geometric and heat transfer parameters combined in the factor Ψ. T_{st} is calculated by the following equation:

$$T_{st} = T_a + \frac{I_T \tau\alpha}{U_2} \qquad (36)$$

$(UA)_4$ is the product of overall heat transfer coefficient and heat transfer area of the condensation region. It is found by the following equation:

$$(UA)_4 = \left(\frac{1}{h_c A_4} + \frac{\ln(D_{co}/D_c)}{2\pi k_c L_4} + \frac{1}{h_w A_{4o}} \right)^{-1} \tag{37}$$

7. Modeling water storage tank

The tank is modeled as a fully mixed tank. This is a reasonable assumption for a tank containing a condenser of parallel vertical tubes. The condenser heats up the water along most of the tank's vertical dimension. It is assumed that the natural convection currents generated along the condenser outer surface will provide the necessary mixing effect in the water and eliminate any thermal stratification.

An energy balance for the tank as a whole can be written as follows:

$$\begin{pmatrix} Heat\ gain\ from \\ condenser \end{pmatrix} \Delta\tau = \begin{pmatrix} Increase\ in\ water \\ internal\ energy \end{pmatrix} + \begin{pmatrix} Heat\ removed\ by \\ water\ withdrawal \end{pmatrix} + \begin{pmatrix} Heat\ losses\ to \\ environment \end{pmatrix} \tag{38}$$

In mathematical form:

$$(Q_4 + Q_5)\Delta\tau = M_w c_{pw}(T_{t2} - T_{t1}) + (Q_w + Q_l)\Delta\tau \tag{39}$$

Solving for the water temperature at the end of the time step T_{t2} gives:

$$T_{t2} = T_{t1} + \frac{\Delta\tau(Q_4 + Q_5 - Q_w - Q_l)}{M_w c_{pw}} \tag{40}$$

Where:

$$Q_w = \dot{m}_w c_{pw}(T_{t1} - T_l) \tag{41}$$

$$Q_l = A_t U_t(T_{t1} - T_a) \tag{42}$$

T_{t2} is then used as an input value or a T_{t1} for the new time step.

8. The iterative procedure

The thermal models described in the previous sections can not be used directly for the estimation of saturation temperature as given by equation (35). The existence of many unknown parameters necessitates the use of a trail and error procedure to solve the problem. The major ***unknowns*** include:

a) Saturation temperature (T_s)

b) Refrigerant mass flow rate (m)

c) Collector subcooled area (A_1)

While the ***known*** parameters are:

a) Solar radiation intensity (I_T)

b) Ambient temperature (T_a)

c) Collector inlet temperature (T_1)

d) Initial storage tank temperature (T_{t1})

Initial guess values of the unknowns are made and corrected several times until the appropriate values that satisfy all equations are attained. A tolerance of 0.0001 is used between the old and calculated values of T_1 , T_{t1} , T_s , $m^{.}$ and any iterated value in the simulation program.

The procedure can be summarized as follows:-

i) The collector subcooled area A_1 is calculated using eq. (2). Accordingly the subcooled length in the collector (L_1) is determined.

ii) The values depending on (L_1) which are (F_1), (h_1) and (A_2) can now be evaluated.

iii) Using (A_2) the boiling rate ($\dot{m}$) can be evaluated from eq. (9).

iv) The calculated (m) from step (iii) is compared with the assumed (m) which is the loop mass flow rate. If they agree within the specified tolerances, calculations proceed, otherwise the new (m) is used to repeat the calculation over and over until convergence is achieved.

v) The refrigerant temperature at collector exit can now be evaluated from eq. (15) depending on the new value of (m) and the assumed saturation temperature (T_s).

vi) Now, a new value of the saturation temperature can be calculated from eq. (35). The new value is compared with the old value used in calculations. If they agree, calculation proceeds, if not, the whole procedure is repeated using the new (T_s) until convergence is achieved.

9. Results and discussion
9.1 Effect of collector fill ratio

Collector fill ratio is easily represented by the ratio of the initial fill length to the total length since the cross sectional area is the same. Fig. 3 shows the variation of tank temperature during the simulation period for various fill ratios. The tank temperature increases with the fill ratio up to a certain optimum which is approximately 0.85 . Increasing the fill ratio means more refrigerant is exposed to solar radiation. This means more heat transfer from the collector to the condenser. However, when the fill ratio is increased beyond the optimum, the condenser does not cope with the large vapor flow by its remaining condensation area. Then the system operates at a higher saturation temperature, the thermal losses from the collector increase resulting in a decrease in collector efficiency. For all

considered fill ratios, the tank temperature increases continuously during the simulation period indicating that heat collection is possible for any fill ratio. Considerable rise in final tank temperature can be noticed (about 38°C) with a fill ratio of 0.5 . Between a fill ratio of 0.5 and the optimum value of 0.85, the additional rise in final tank temperature is within 10 ^{o}C. Increasing the fill ratio beyond 0.85 causes a reduction of about 5 ^{o}C in the final tank temperature.
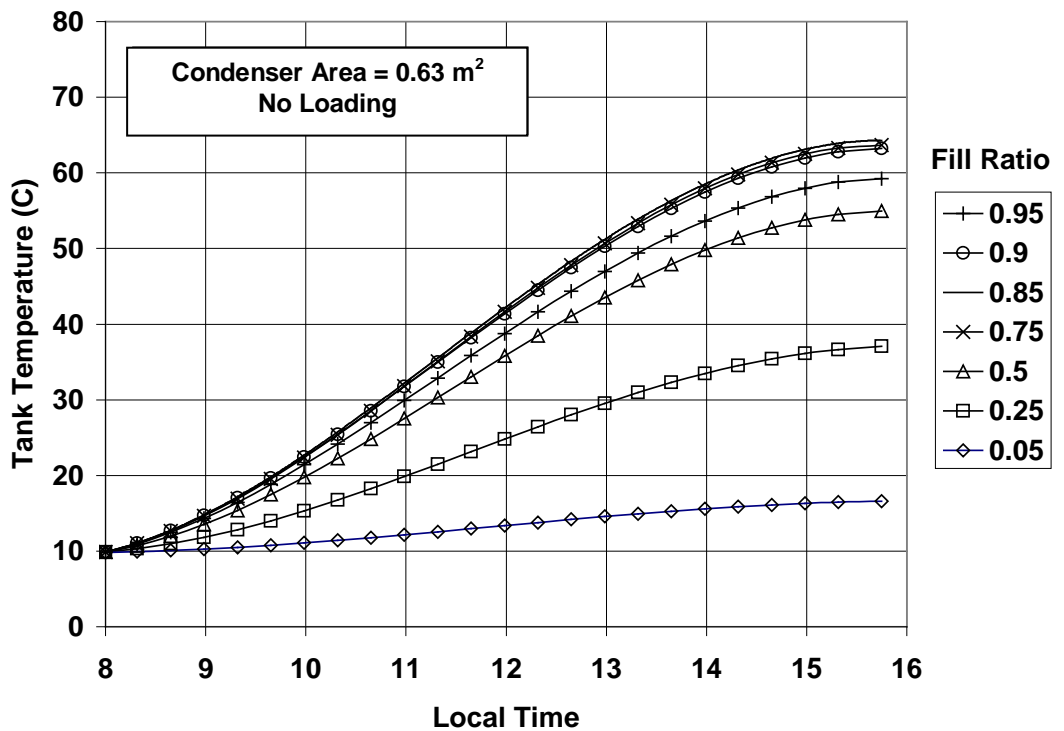
Fig. (3) Variation of storage water temperature during the simulation period for various fill ratios.
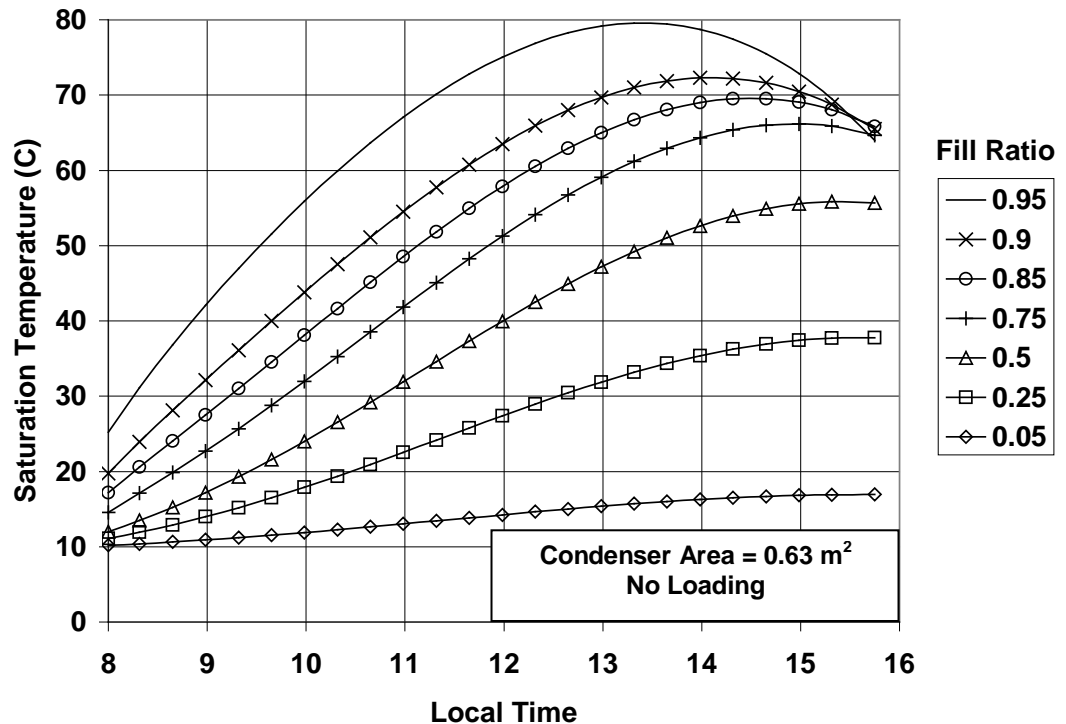
Fig. (4) Variation of system saturation temperatures during the simulation period for various fill ratios.

Fig. 4 shows the variation of the system saturation temperature for the same range of fill ratios from 0.05 to 0.95. The system saturation temperature increases with fill ratio and improves heat collection because the condenser will deliver heat to the storage water at a higher temperature which increases the final tank temperature and the collector efficiency. This is true only up to the optimum fill ratio, after which increasing the saturation temperature causes a reduction in the final tank temperature. A higher saturation temperature results in increased thermal losses. This loss is not counter balanced by the condenser. The increment in the stored heat will be less than the increment in the collector losses for the same saturation temperature.

Fig. 5 gives the final saturation and tank temperatures from Figs. 3 and 4 at the end of the simulation period as a function of the fill ratio. Despite the narrow difference between the saturation and tank temperatures, the estimated value of condensation heat transfer coefficient and condensation area will compensate the low temperature difference and ensure the completion of condensation. However, the above narrow difference occurs only at the final period of the simulation. The difference between saturation and tank temperatures is greater at the beginning and middle of the simulated period.

Fig. 6 shows the variation of the collector efficiency during the simulation period for the fill ratios considered. The collector efficiency increases with fill ratio up to the optimum and starts to decease beyond that. The collector efficiency exhibits a slight increase before 10:30

a.m. then starts to decrease till the end of the simulation period. This is caused by increased collector thermal losses at higher saturation temperatures.

Collector efficiency is equivalent to the system efficiency in the present work. Because the useful heat gain of the collector is equal to the storage tank heat gain when the connecting pipes and tank thermal losses are ignored. Any increase in heat storage means better collection in the collector. Therefore, the collector efficiency will be used as a measure of the system performance as a whole.
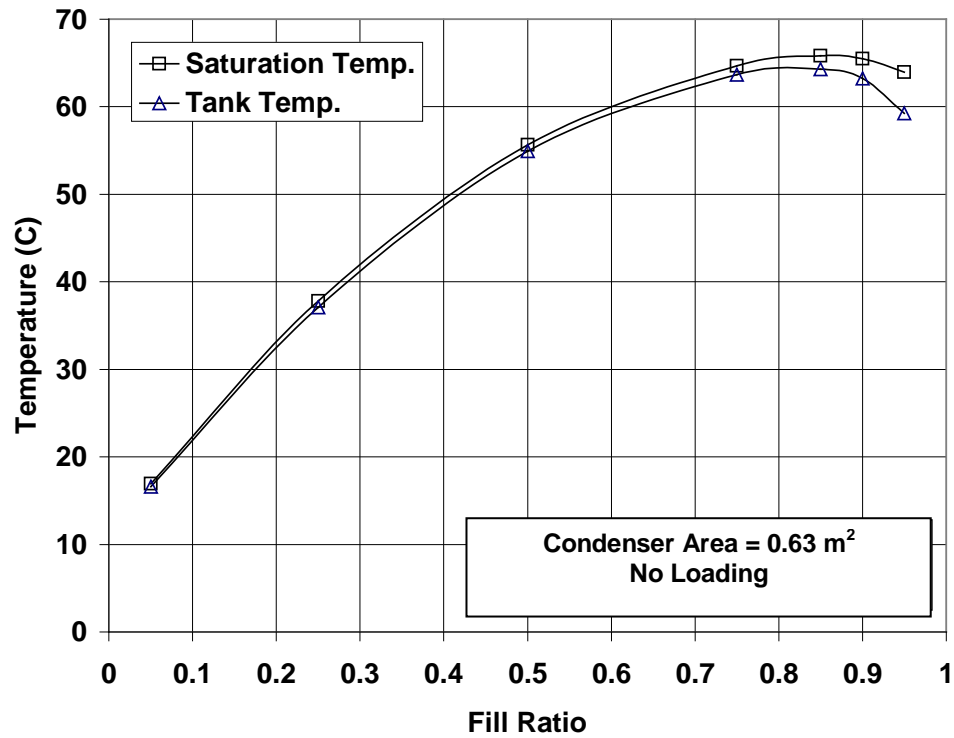
Fig. (5) Variation of final tank and system saturation temperatures with fill ratio.
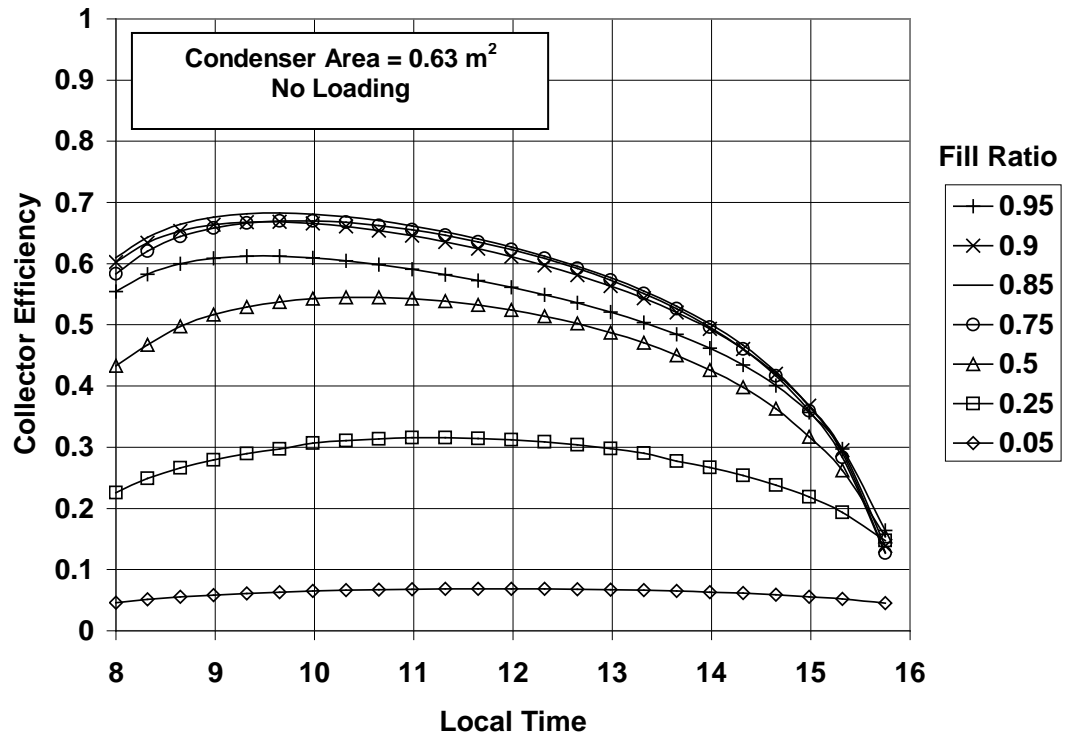
Fig. (6) Variation of collector efficiency during the simulation period for various fill ratios.

The existence of an optimum fill ratio was reported by other researchers [12, 17, and 18]. However, different optimum fill ratios were reported which ranged between 40-80%. The optimum fill ratio is a strong function of the location of the condenser. So, the change of the condenser location relative to the evaporator (or the solar collector) changes the optimum system fill ratio. McDonald et al. [17] suggested that the optimum fill ratio is achieved when the refrigerant does not flood the condenser anywhere.

9.2 Effect of condenser area

The condenser area is the inside wall area of the condenser pipes. It is seen from Fig. 7 that the tank temperature always increases with the condenser area. Increasing the condenser area induces the system to adapt itself by decreasing the saturation temperature as shown in Fig. 8. When the system operates at a lower saturation temperature, the collector works at a higher efficiency which means better heat collection and a higher tank temperature. Heat collection in flat-plate solar collectors should always be done at the lowest possible temperature in order to ensure that the collector works at the highest possible efficiency. Price et al. [7] reported that increasing the boiling collector absorber temperature leads to a reduction in collector efficiency. The absorber plate temperature, as they reported, increases when a dry-out condition occurs in the superheated region of the collector.

The saturation temperature variation follows the tank temperature by increasing continuously during the simulation period. But this trend was not witnessed for all condenser areas. For condenser areas below 0.63 m^2 the saturation temperature does not follow the tank temperature after 1:30 p.m. Rather, it decreases slightly towards the end of the simulation period. The decrease becomes larger for lesser condenser areas as seen in Fig. 8.

The change of the condenser area in the present work was simulated by changing the number of condenser pipes. The cross sectional area and the height of each pipe were kept unchanged for all the condenser areas considered in the simulations. In this way, the location of the condenser relative to the solar collector did not change when the condenser area was changed.
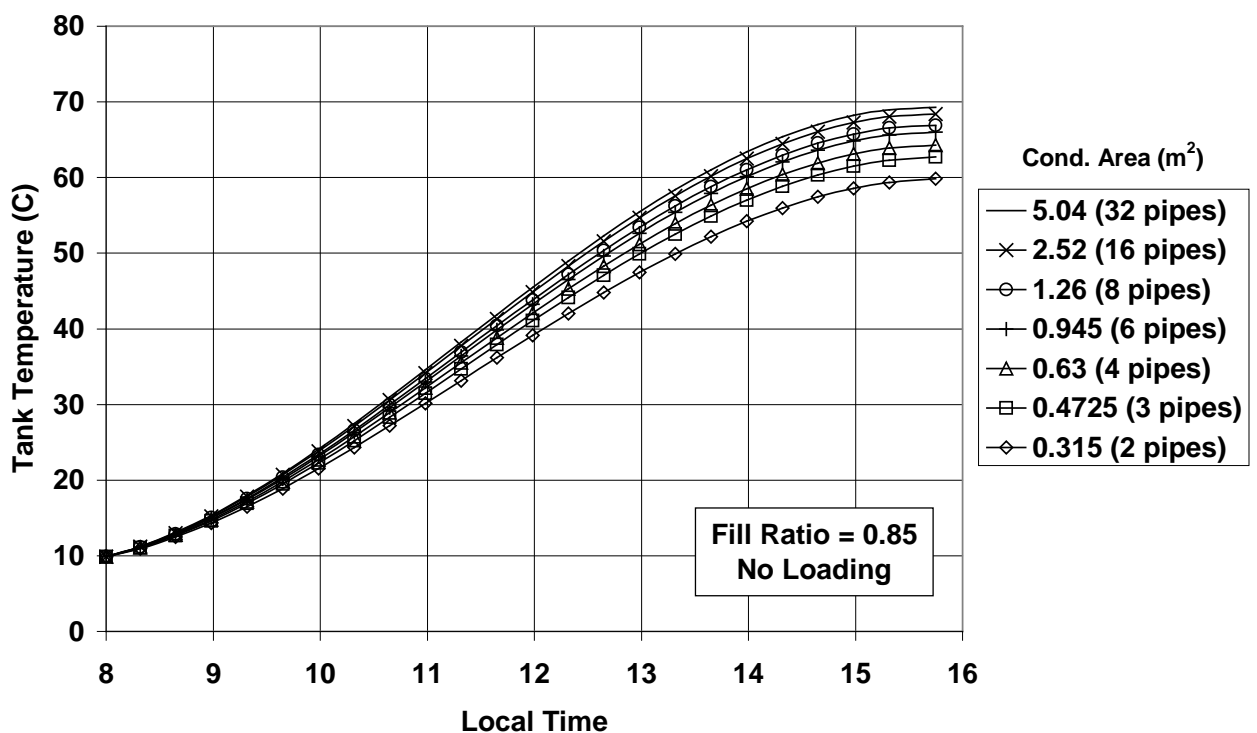
Fig. (7) Variation of storage water temperature in the simulation period for various condenser areas.
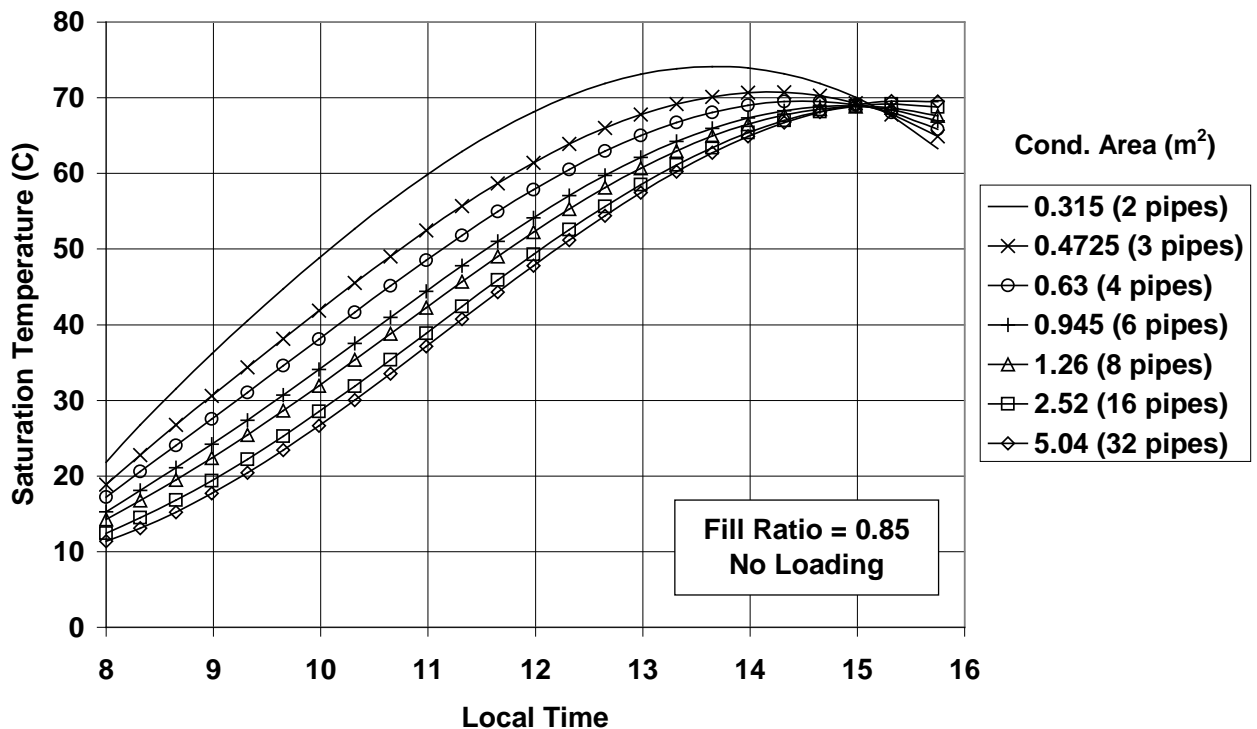
Fig. (8) Variation of system saturation temperatures during the simulation period for various condenser areas.

The effect of condenser area on the final tank and the final system saturation temperatures at the end of the simulation period is shown in Fig. 9. Increasing the condenser area beyond a certain value (1.5 m^2) does not significantly increase the final tank temperature. However, decreasing the condenser area less than 0.05 m^2 deteriorates the system performance. Fig. 9 shows that for condenser areas less than 0.05 m^2 the final tank temperature sharply decreases and the saturation temperature sharply increases. This is interpreted as a type of choking in the loop. For condenser areas below 0.05 m^2, the system is not capable of delivering the collected energy with this small area. So, the system adapts itself by increasing the saturation temperature such that the temperature difference between the condenser and the tank is just enough to deliver the heat. However, a high saturation temperature increases the collector thermal losses which decreases the collection of heat resulting in a decreased final tank temperature.

The change of collector efficiency with condenser area is less pronounced than the change of collector efficiency with fill ratio as can be deduced by comparing Figs. 6 and 10.
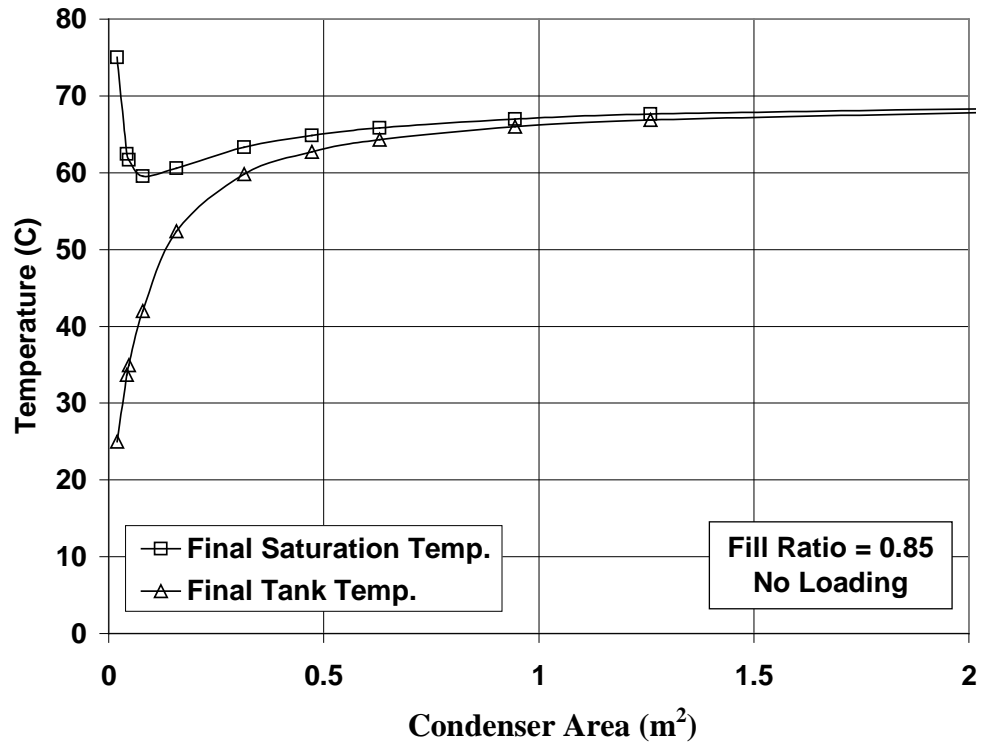
Fig. (9) Variation of final tank and saturation temperatures with condenser area.
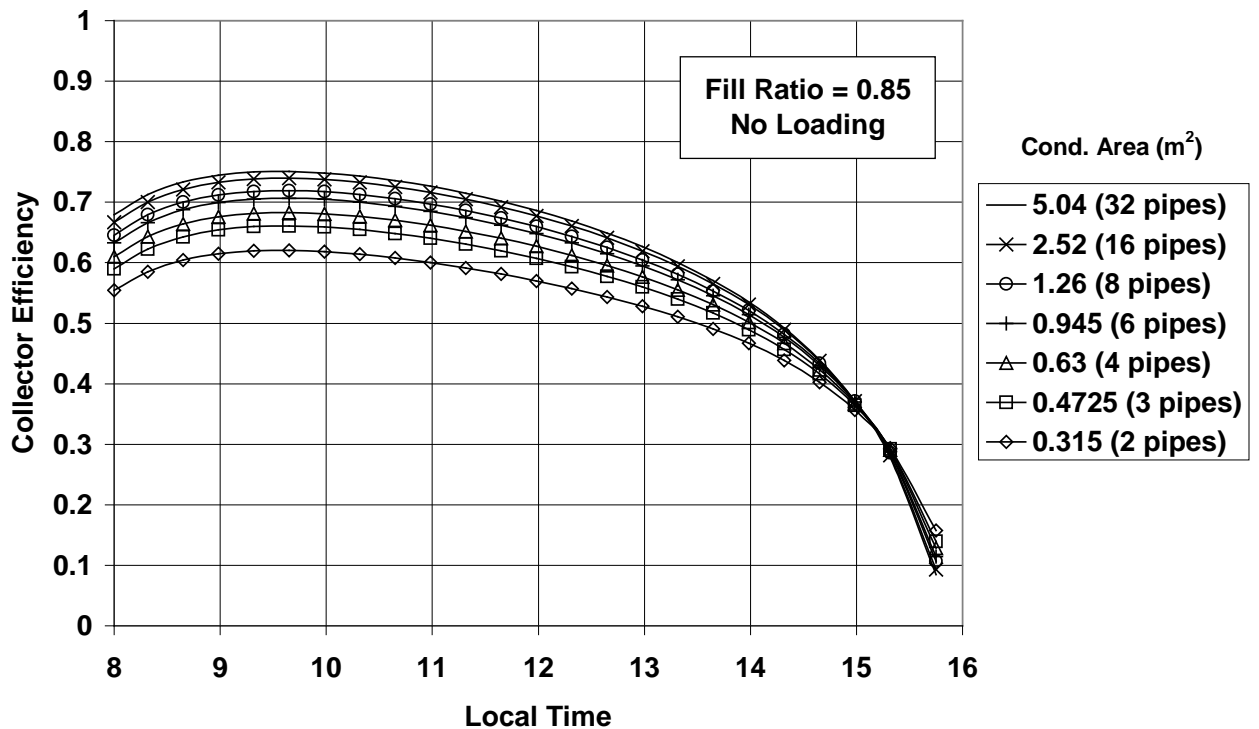
Fig. (10) Variation of collector efficiency during the simulation period for various condenser areas.
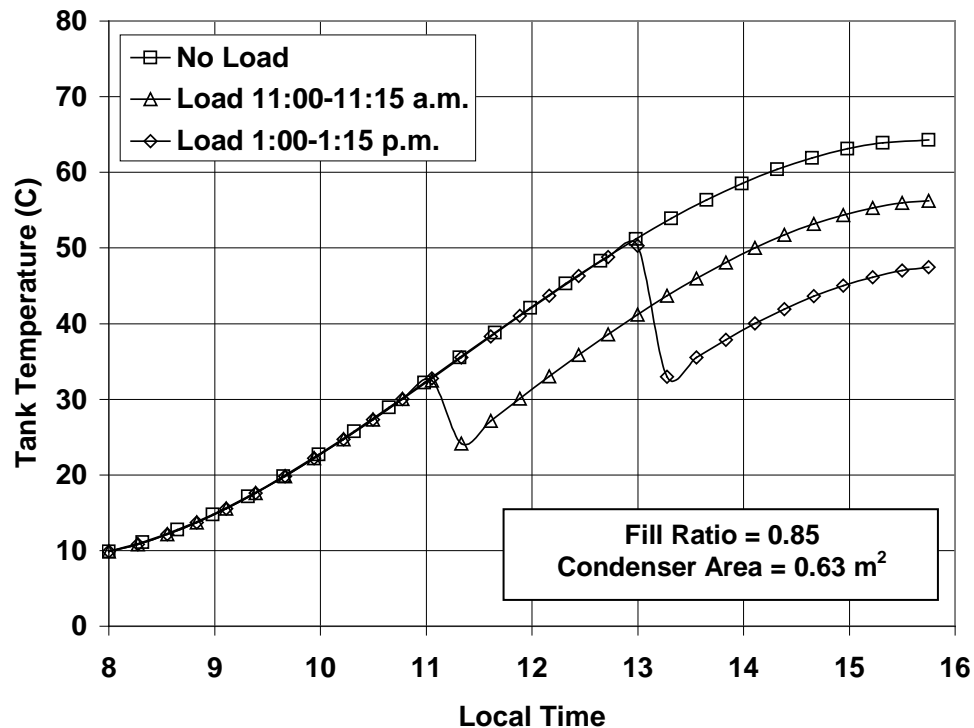
Fig. (11) Variation of tank temperature for three loading conditions.

9.3 Effect of tank loading

Tank loading causes a sharp decrease in tank temperature because the withdrawn hot water is replaced by an equal quantity of cold water at $10^{o}C$ as shown in Fig. 11. Two patterns of water withdrawal were applied in the simulations. In both patterns the water withdrawal was at a continuous rate of 0.08 kg/s during each 15 minutes of the loading periods. This value of loading rate represents a typical tap flow rate. In the first pattern, water is withdrawn from the tank between 11:00 and 11:15 a.m. (in the first half of the day). The second pattern assumes the withdrawal to be carried out between 1:00 and 1:15 p.m. (in the second half of the day).

The saturation temperature was seen to follow the tank temperature in all the simulations, with a slight difference at the end of the simulation period as shown in Fig. 12. Since the tank temperature decreases during loading, the saturation temperature also decreases. This makes the collector operate at a lower temperature, hence, at a higher efficiency as shown in Fig. 13.

The decrease in the saturation and tank temperatures is more pronounced in the second loading period (1:00 to 1:15 p.m.) than in the first loading period (11:00 to 11:15 a.m.). This is because the withdrawn water in the second period is at a higher temperature and contains a larger amount of energy. Therefore it represents a larger loss to the system. It can be seen from Fig. 11 that the early loading gives the system longer time to compensate the lost heat than in the case of late loading. So, the final tank temperature for the case of early loading will be higher than that of the late loading.
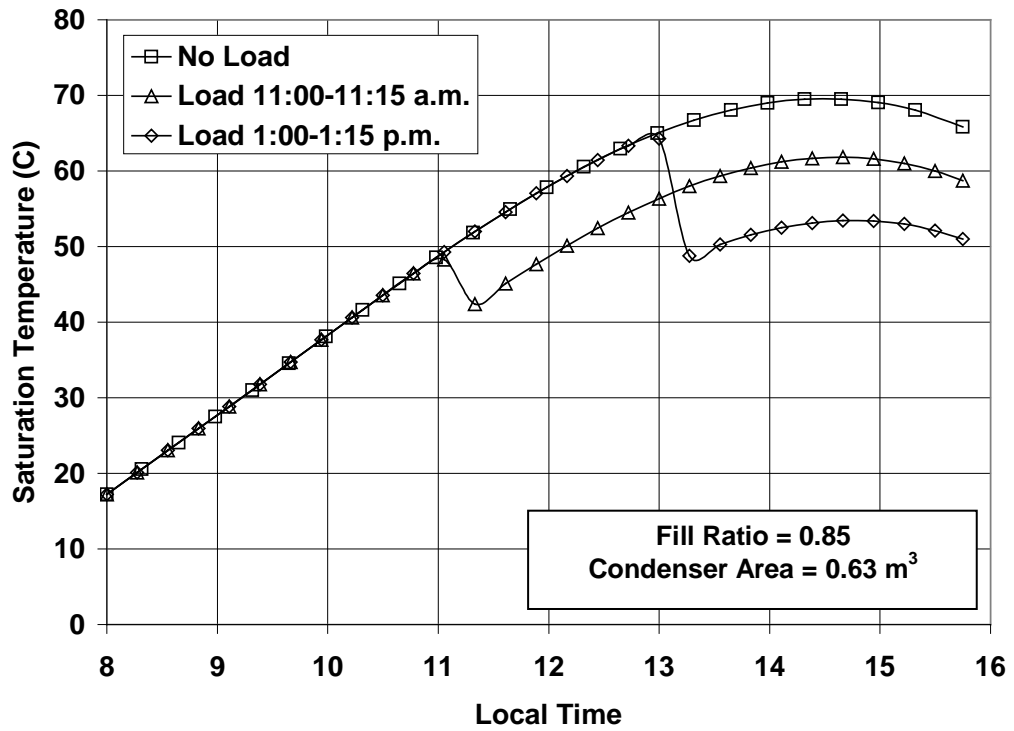
Fig. (12) Variation of system saturation temperature for three loading conditions.
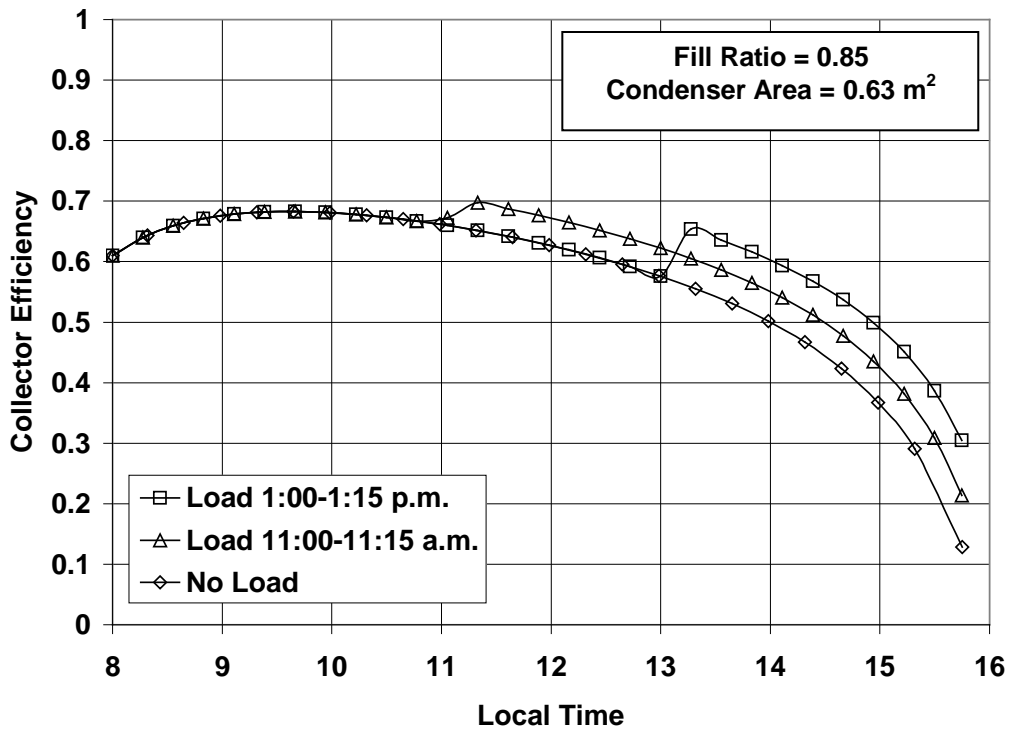
Fig. (13) Variation of collector efficiency for three loading conditions.

Fig. 14 shows a comparison between the present theoretical results and the experimental data of Downing and Walden [2]. The comparison was done using a fixed mass flow rate of 0.01 kg/s which is the value adopted by Downing and Walden in their experiments. Fig. 14 depicts three collector efficiency lines; one is experimental and the other two lines are generated by the computer simulation program of the present study for fixed and variable refrigerant mass flow rates. Table (2) shows the system characteristics adopted by Ref. [2].
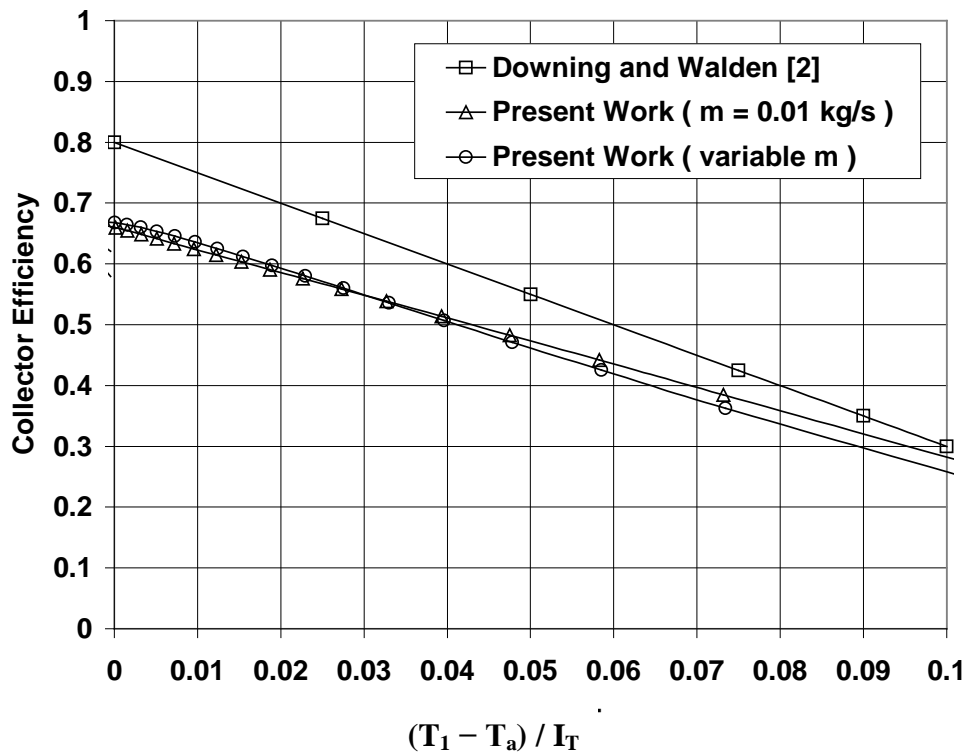
Fig. (14) Comparison between the present work and ref. [2].

Table (2): System characteristics of ref. [2].

Collector	Dimensions (width×length)	1.7×2.5	m
	Inside Pipe Diameter	0.012	m
	Outside Pipe Diameter	0.014	m
	Number of pipes	15	
	Fill ratio	0.75	
	Tilt Angle	50°	
	Top Heat Loss Coeff.	5	$W/(m^2\,{}^{o}C)$
	Tα	0.8	
Storage	Volume	0.3	m^3
	Loss Coefficient	0.5	$W/(m^2\,{}^{o}C)$
Condenser	Inside Area	2	m^2
	Inside Pipe Diameter	0.0254	m
	Pipe Thickness	.001	m
	Pipe Height	1.05	m
	Number of Pipes	24	

10. Conclusions

i) The tank temperature increases with the collector fill ratio until an optimum limit of approximately 0.85 .

ii) The collection of heat is possible at any fill ratio. Maximum tank temperature of 64 ^{o}C was achieved at a fill ratio of 0.85 in December.

iii) Collector efficiency increases with fill ratio till the optimum.

iv) The saturation temperature decreased with increasing condenser area. this renders the collector to work at a higher efficiency leading to a higher tank temperature. When the condenser area was increased from 0.63 m^2 to 2.52 m^2 the final tank temperature increased about 5°C. The maximum condenser area is restricted only by the space available inside the water storage tank.

v) For a condenser area of less than 0.05 m^2 a chocking phenomenon was observed in the system where the saturation temperature sharply increased and the tank temperature sharply decreased.

vi) Loading the system for 15 minutes before noon caused a decrease in the final tank temperature by about 8 ^{o}C and by about 18 ^{o}C with the afternoon loading.

vii) The collector efficiency increased by 7% with morning loading and 10% with afternoon loading.

11. References

[1] Soin, R. S., Rao, K. S., Rao, D. P., and Rao, K. S., "*Performance of flat-plate solar collector with fluid undergoing phase change*", Solar Energy, Vol. 23, pp. 69-73, 1979.

[2] Downing, R. C., and Walden, V. W., "**Phase-change heat transfer in solar hot water heating system using R-11 and R-114",** ASHRAE Transactions, Vol. 86, Part I, 1980.

[3] Schreyer, J. M., "*Residential application of refrigerant charged solar collectors*", Solar Energy, Vol. 26, pp. 307-312, 1981.

[4] Al-Tamimi, A. I., and Clark, J. A., "*Thermal analysis of a solar collector containing a boiling fluid*", Proceedings of the 1983 annual meeting of the American Solar Energy Society, Minneapolis, MN, June 1-3, 1983.

[5] El-Assy, A. Y., and Clark, J. A., "T*hermal analysis of a flat-plate collector in multiphase flows, including superheat",* Solar Energy, Vol. 40, No. 4, pp. 345-361, 1988.

[6] Abramzon, B., Yaron, I., and Borde, I., "*An analysis of a flat-plate solar collector with internal boiling*", ASME J. Solar Energy Engineering, Vol. 105, pp. 454-460, Nov. 1983.

[7] Price, H. W., Klein, S. A., Beckman, W. A., "*Analysis of boiling flat-plate collectors*", ASME J. Solar Energy Engineering, Vol. 108, pp. 150-157, May 1986.

[8] Fanney, A. H., and Terlizzi, C. P., "*Testing of refrigerant-charged solar domestic hot water systems*", Solar Energy, Vol. 35, No. 4, pp. 353-366.

[9] Radhwan, A. M., Zaki, G. M., and Jamil A., "*Refrigerant-charged integrated solar water heater",* Intl. J. Energy Research, Vol. 14, pp. 421-432, 1990.

[10] Pluta, Z., and Pomierny, W., *"The theoretical and experimental investigation of the phase-change solar thermosyphon",* Renewable Energy, Vol. 6, No. 3, pp. 317-321, 1995.

[11] Joudi, K. A., and Al-Tabbakh, A. A., "*Computer simulation of a two phase Thermosyphon solar domestic hot water heating system*", Energy Conversion and Management, Vol. 40, pp. 775-793, 1999.

[12] Lin, M. C., Chun, L. J., Lee, W. S., and Chen, S. L., "*Thermal performance of a two phase thermosyphon energy storage system",* Solar Energy, Vol. 75, pp. 295-306, 2003.

[13] Esen, M., and Esen, H., "*Experimental investigation of a two-phase closed Thermosyphon solar water heater",* Solar Energy, Vol. 79, pp. 459-468, 2005.

[14] ASHRAE Handbook, Fundamentals, 1985.

[15] Hsieh, J. S., "*Solar Energy Engineering",* Prentice-Hall Inc., 1986.

[16] Van der Walt, J., and Kroger, D. G., "*Heat transfer during film condensation of saturated and superheated Freon-12",* Prog. Heat Mass Transfer, Vol. 6, pp. 75-98, 1972.

[17] McDonald, T. W., Hwang, K. S., and Diciccio, R., *"Thermosyphon loop performance characteristics: Part 1. Experimental study"* ASHRAE Transactions, Vol. 83, Part II, pp. 250, 1977.

[18] Ali, A. F. M., and McDonald, T. W., *"Thermosyphon loop performance characteristics: Part 2. Simulation program"* ASHRAE Transactions, Vol. 83, Part II, pp. 260, 1977.

[19] Rohsenow, W. M., "*A method of correlating heat transfer data for surface boiling liquids"*, Transactions of ASME, Vol. 74, pp. 969-976, 1952.